TECHNOLOGY AND PRACTICE OF THE ROOF-CAVING OF HYDRAULIC FRACTURING IN A FULLY MECHANIZED CAVING FACE

by

Qigen DENG[a,b,c*], Fajun ZHAO[a,b], Hong LI[b], Jingping YIN[b], Tao ZHANG[b], and Junjie WEI[b]

[a] State Key Laboratory Cultivation Base for Gas Geology and Gas Control, Henan Polytechnic University, Jiaozuo, Henan, China
[b] School of Safety Science and Engineering, Henan Polytechnic University, Jiaozuo, Henan, China
[c] State Collaborative Innovation Center of Coal Work Safety and Clean-Efficiency Utilization, Jiaozuo, Henan, China

Original scientific paper
https://doi.org/10.2298/TSCI191104096D

A fracture expansion criterion of hydraulic fracturing was suggested to deal with the hard and stable roof control in coal mines. An experiment was designed for the roof control, and the reliability of model was verified. Four different types of fracturing holes and fracturing technology were designed in the setup room, and the hydraulic fracturing in the roof of a fully mechanized caving face was implemented.

Key words: *hard and stable roof, hydraulic fracturing, fracturing model, borehole, underground test*

Introduction

High strength, undeveloped joint crack, large thickness, strong integrity and self-supporting ability are the main characters of hard roof rock in coal mine. After mining, the roof rock will be exposed in the goaf and will not fall in a short period of time. Once the collapse occurs, a large collapsed area is predicted, and there is a strong periodic pressure. There is obvious dynamic phenomenon when pressure outcomes, which often results in equipment damage and gas disaster accidents [1-3]. About one third of the coal seams in China belong to hard and stable roofs which are difficult to be collapsed, and they are distributed in more than 50% of the mining areas. At present, deep-hole blasting is the main method to control hard and difficult collapse roof in China, and water injection softening is the supplementary method. Although the technology and process of deep-hole blasting are matured and they are flexible in operation, however, it is difficult to deal with blow-out shot, moreover, the vibration is harmful and the roof collapse area is difficult to be predicted and to be controlled. The failure of operation may lead to open fire in blasting, which may easily lead to gas overrun accident or gas explosion accident caused by instantaneous pressure of gas in goaf [4, 5].

Directional hydraulic fracturing technology can solve effectively the problems faced by deep hole blasting and it is conducive for resource recovery of coal mine [5, 6]. Poland

* Corresponding author, e-mail: dengqigen@hpu.edu.cn

was the first country where the hydraulic fracturing technology was applied to the treatment and control of underground hard roof in coal mines. Later, scholars carried out research on the application of hydraulic fracturing technology in coal mines, analyzed the mechanism of hydraulic fracturing treatment of hard roof, gave the conditions of hydraulic fracture initiation and expansion, and proposed the mechanism to achieve directional stratification of roof hydraulic fracturing. The influencing factors and rules of hydraulic fracture propagation were studied both numerically and experimentally. In recent years, hydraulic fracturing technology has been widely used in the development of low permeability oil and gas reservoirs, the control of hard roof, gas permeability enhancement, dynamic pressure roadway pressure relief and other fields [1-3, 5, 7].

Theory and technology of hydraulic fracturing

It is considered that the plastic yield and shear dilatancy of rock have influence on the rock cracking of hydraulic fracturing, and the plastic yield near the crack tip leads to an effective yielding [7]. Hard rock is often regarded as a kind of brittle materials. The stress field of the surrounding rock mass, the structural characteristics and mechanical properties of the coal and rock mass determine the pressure parameters of the hydraulic fracturing and the expansion and extension of the crack propagation. It is generally believed that in the original coal and rock mass of 200-600 m in the shallow part, the external pressure water cracks at the minimum horizontal stress and forms the vertical main crack [8, 9]. Under the continuous impact of external high pressure water, an extended-airfoil branching fracture pattern was formed, the water gradually extends to the deep part of coal and rock mass. In this process, water gradually infiltrates into the coal and rock mass through the main fissures and airfoil fissures, which enlarge the water-coal rock contact surface. When the coal-rock contact surface is wetted by the larger contact angle of the water body, the water content of the coal and rock mass increases, and then the coal and rock mass are wetted and softened, so as to achieve the effect of structural transformation of coal-rock mass, slight weakening and improving the connection between the fissures [10, 11].

Hydraulic fracture generally propagates along the direction perpendicular to the minimum principal stress. If the vertical principal stress, σ_v, is greater than the minimum horizontal principal stress, σ_h, a vertical fracture will be formed, as shown in fig. 1. If the vertical principal stress, σ_v, is less than the minimum horizontal principal stress, σ_h, horizontal cracks will be formed, shown in fig. 2 [12-16].

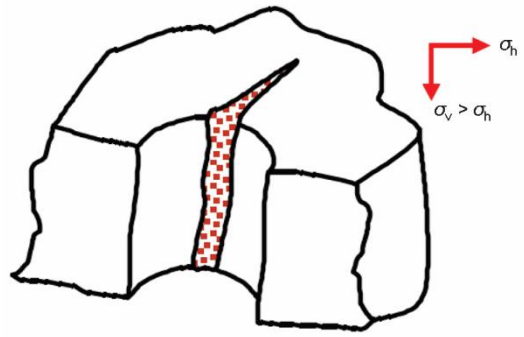

Figure 1. Diagram of vertical fracture

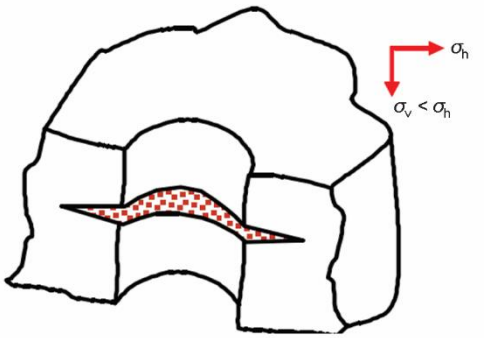

Figure 2. Diagram of horizontal fracture

In the 2-D model of fracture propagation, many KGD, PKN and Penny-Shaped models were established, which are the most representative and widely used of fracture models. Sneddon gave a simpler coin model based on the above model, it can see in fig. 3 [17-20], where R and W represent the length and width of cracks, respectively, Q – the inject liquid, and P – the water pressure.

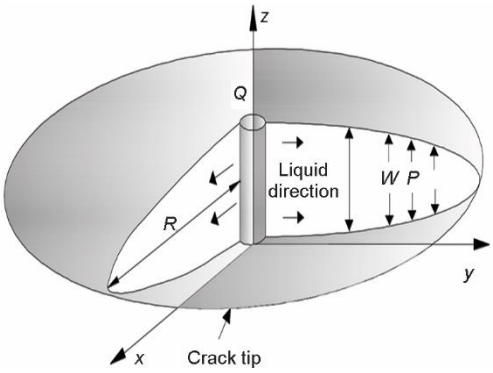

Figure 3. Fracture model of Penny-Shape

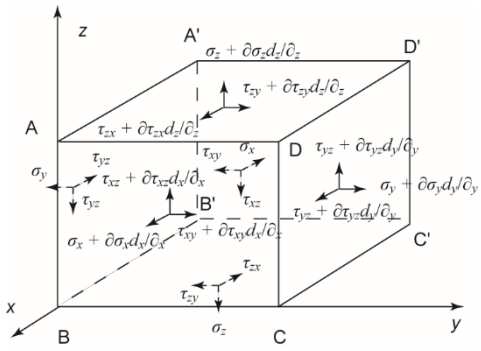

Figure 4. Mechanics model of micro rock

Pressure of hydraulic fracturing

Arbitrarily selected a parallelogram hexahedral element ABCDA'B'C'D' in the roof rock mass of the working face and the modeling as shown in fig. 4 [21-24].

Assuming that d_x, d_y, and d_z are the edge lengths of the element, the surface force components are F_x, F_y, and F_z, the maximum principal stress is the same as the x-axis, the minimum principal stress is the same as the z-axis, the forces on other surfaces are shown in tab. 1.

The balance equations in the x-, y-, and z-axis directions are shown in eq. (1):

$$\begin{aligned}
&\left(\sigma_x+\frac{\partial\sigma_x}{\partial_x d_x}\right)d_y d_z+\left(\tau_{yz}+\frac{\partial\tau_{yz}}{\partial_y d_y}\right)d_x d_z+\left(\tau_{zx}+\frac{\partial\tau_{zx}}{\partial_z d_z}\right)d_x d_y+\\
&+F_x d_x d_y d_z=\sigma_x d_y d_z+\tau_{yz}d_x d_z+\tau_{zx}d_x d_y\\
&\left(\tau_{xy}+\frac{\partial\tau_{xy}}{\partial_x d_x}\right)d_y d_z+\left(\sigma_y+\frac{\partial\sigma_y}{\partial_y d_y}\right)d_x d_z+\left(\tau_{zy}+\frac{\partial\tau_{zy}}{\partial_z d_z}\right)d_x d_z+\\
&+F_y d_x d_y d_z=\tau_{xy}d_y d_z+\sigma_y d_x d_z+\tau_{zy}d_x d_y\\
&\left(\sigma_z+\frac{\partial\sigma_z}{\partial_z d_z}\right)d_x d_y+\left(\tau_{yz}+\frac{\partial\tau_{yz}}{\partial_y d_y}\right)d_x d_z+\left(\tau_{xz}+\frac{\partial\tau_{xz}}{\partial_x d_x}\right)d_y d_z+\\
&+F_z d_x d_y d_z=\tau_{xz}d_y d_z+\tau_{yz}d_x d_z+\sigma_z d_x d_y
\end{aligned}\tag{1}$$

In eq. (1), divide all terms by $d_x d_y d_z$, the Navier equation can be obtained, it shows in eq. (2):

$$\begin{aligned}
\frac{\partial \sigma_x}{\partial x} + \frac{\partial \tau_{yx}}{\partial y} + \frac{\partial \tau_{zx}}{\partial z} + F_x = 0 \\
\frac{\partial \tau_{xy}}{\partial x} + \frac{\partial \sigma_y}{\partial y} + \frac{\partial \tau_{zy}}{\partial z} + F_y = 0 \\
\frac{\partial \tau_{xz}}{\partial x} + \frac{\partial \tau_{yz}}{\partial y} + \frac{\partial \sigma_z}{\partial z} + F_z = 0
\end{aligned} \tag{2}$$

Table 1. Stress distribution of micro rock

Plane name	Square	Stress projection		
		x-axis	*y*-axis	*z*-axis
ABCD	$d_y d_z$	$\frac{\sigma_x + \partial \sigma_x}{\partial_x d_x}$	$\frac{\tau_{xy} + \partial \tau_{xy}}{\partial_x d_x}$	$\frac{\tau_{xz} + \partial \tau_{xz}}{\partial_x d_x}$
A'B'C'D'	$d_y d_z$	σ_x	τ_{xy}	τ_{xz}
C'D'DC	$d_x d_z$	$\frac{\tau_{vz} + \partial \tau_{vz}}{\partial_v d_v}$	$\frac{\sigma_y + \partial \sigma_y}{\partial_y d_y}$	$\frac{\tau_{yz} + \partial \tau_{yz}}{\partial_y d_y}$
ABA'B'	$d_x d_z$	τ_{yz}	σ_y	τ_{yz}
BCC'B'	$d_x d_y$	$\frac{\tau_{zx} + \partial \tau_{zx}}{\partial_z d_z}$	$\frac{\tau_{zy} + \partial \tau_{zy}}{\partial_z d_z}$	$\frac{\sigma_z + \partial \sigma_z}{\partial_z d_z}$
AA'D'D	$d_x d_y$	τ_{zx}	τ_{zy}	σ_z

From eq. (1), the first principal stress σ_1, the second principal stress σ_2 and the third principal stress σ_3 can be obtained, as shown in eq. (3):

$$\begin{aligned}
\sigma_1 &= \sigma_x d_y d_z + \tau_{yz} d_x d_z + \tau_{zx} d_x d_y \\
\sigma_2 &= \tau_{xy} d_y d_z + \sigma_y d_x d_z + \tau_{zy} d_x d_y \\
\sigma_3 &= \tau_{xz} d_y d_z + \tau_{yz} d_x d_z + \sigma_z d_x d_y
\end{aligned} \tag{3}$$

When the mining depth of a mine is less than 1000 m, the vertical stress can be regarded as the third principal stress, $\sigma_3 = \sigma_z$.

When the internal friction angle of rock is θ, the uniaxial compressive strength is σ_c, the cohesion is c. By simplifying Mohr-Coulomb strength theory, eq. (4) into eq. (3), the eq. (5) can be obtained:

$$\sigma_1 = \sigma_3 \frac{1+\sin\theta}{1-\sin\theta} + \sigma_c \tag{4}$$

$$\left(\sigma_x - \tau_{xz}\frac{1+\sin\theta}{1-\sin\theta}\right) d_y d_z + \left(\tau_{yz} - \tau_{zy}\frac{1+\sin\theta}{1-\sin\theta}\right) d_x d_z + \left(\tau_{zx} - \sigma_z \frac{1+\sin\theta}{1-\sin\theta}\right) d_x d_y = \sigma_c \tag{5}$$

The direction of τ_{xz}, τ_{yz}, and τ_{zx} along the x-axis or z-axis all cause damage or displacement in fig. 4, According to the fracture model in fig. 3, when W develops on the z-axis of the microelement, τ_{xz}, τ_{yz}, and τ_{zx} are the ultimate shear stresses. Assumption: fig. 4 is a homogeneous body, then $\tau_{xz} = \tau_{yz} = \tau_{zx}$ at the time of failure. The τ_{zy} does not destroy the micro-

element along the *y*-axis, and τ_{zy} is very small, making $\tau_{zy} = 0$. Take $d_x = d_y$ as unit length 1. By eliminating the first principal stress in eq. (5) with eq. (4), the eq. (6) can be obtained:

$$\left(\sigma_z \frac{1+\sin\theta}{1-\sin\theta} - \tau_{xz} \frac{2}{1-\sin\theta}\right) d_z + \tau_{xz} - \sigma_z \frac{1+\sin\theta}{1-\sin\theta} = \sigma_c \tag{6}$$

Shear force is separated from eq. (6), it can get:

$$\tau_{xz} = \frac{1-\sin\theta}{2d_z + \sin\theta - 1}\left[\sigma_c + \sigma_z \frac{(1+\sin\theta)(d_z - 1)}{1-\sin\theta}\right] \tag{7}$$

Define τ_{xz} [MPa] as the shear stress caused by hydraulic fracture, the d_z [m] is defined as the fracture width, and C [MPa] is the cohesion of rock. From the Coulomb strength line, the hydraulic fracturing pressure can be obtained.

$$P = \left\{\frac{1-\sin\theta}{2d_z + \sin\theta - 1}\left[\sigma_c + \sigma_z \frac{(1+\sin\theta)(d_z - 1)}{1-\sin\theta}\right] - C\right\} / \tan\theta \tag{8}$$

Assuming that the vertical stress is the third principal stress, and the direction of the fracture is perpendicular to the direction of the minimum principal stress, so the direction of the hydraulic fracture is along the direction of the rock layer (x, y). The eq. (8) shows that the pressure of hydraulic fracturing is affected by the fracture of rock layer. The vertical stress is linearly related to the hydraulic fracturing pressure, and the pressure required for hydraulic fracturing increases with the increase of mining depth.

Hydraulic fracturing practice

The test site is located in the southeastern margin of Qinshui Basin, Shanxi Province, China. Test area of the roadway ventilation section of 1310 fully mechanized caving face is rectangular, its width is 4.2 m, its height is 2.6 m, its cross-section area is 10.92 m^2. The No. 3 coal seam is mining seam, the average depth of coal seam is 431 m, the average thickness of coal seam is 6.3 m, and the inclination angle of coal seam is 1-3°, the average is 1.5°. The main roof of coal seam is medium-sized sandstone with a thickness of 6.13 m. The bedding is well developed. It contains many muscovite sheets and siderite Oolitic. The sand bodies are overlapped in flower shape and are mostly inverse grain sequence. It has medium-sized and small-sized staggered and vein-like bedding and wavy bedding. It belongs to medium-hard rock. Most of them are sandy mudstone in the immediate roof, some are mudstone and siltstone with a thickness of 4.15 m. Cracks are not well developed, coal line is not well developed, and sandy material is unevenly distributed, which belongs to weak rock. The level of in-situ stress belongs to the low-soil stress area, which is generally $\sigma_H > \sigma_V > \sigma_h$ stress field, mainly composed of tectonic stress.

Hydraulic fracturing technology and process

Fracturing hole drilling: The drilling machine with good mobility, high stability and fast drilling speed is used to hole drilling in the roof of the roadway. After drilling, the whole borehole should be washed with hydrostatic water.

Hole sealing: Connect the accumulator, manual pump and hose and the other end of the hose that will be sent to the borehole. Use manual pump to pressurize the packer to expand the packer hose and achieve the purpose of sealing, as shown in fig. 5(a).

Fracturing: High pressure winding hose is used to connect the high pressure pump with the high pressure water injection steel pipe, open the high pressure pump, high pressure water enters the sealing section, the water pressure of the sealing section decreases after fracturing, and then enters the holding stage (usually no less than 30 minutes). At this stage, crack growth is accompanied by new cracks. Flow meters are used to monitor flow and injected water to ensure that roof strata are fully weakened and softened until the fracturing is completed, as shown in fig. 5(b).

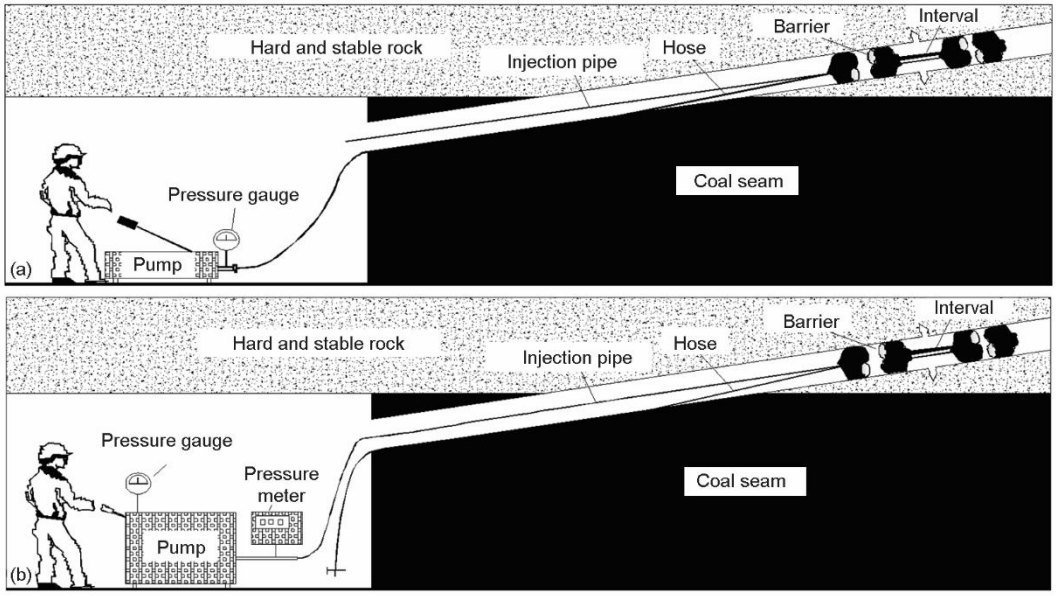

Figure 5. Technological process of hydraulic fracturing; (a) hole sealing and (b) water injection to fracturing

Hydraulic fracturing construction parameters and fracturing pump selection

The borehole is drilled with a diameter-preserving and reinforcing bit with a diameter of Ø56 mm. Two types of fracturing boreholes, *S* and *L*, are arranged in the setup room. The drilling and fracturing operations of the fracturing borehole, *L*, are performed first, and then the fracturing and drilling, *S*, construction and fracturing operations are performed. Two types of borehole, *A* and *J*, are arranged in the upper and lower two lanes. The borehole *A* parallel roadway is set in the direction of the goaf. First, the drilling and fracturing operations of the fracturing borehole *J* are carried out, then the fracturing borehole *A* construction and fracturing operations are carried out. The schematic diagrams of the *S*, *L* drilling arrangements are shown in figs. 6-8, respectively. The spacing of each borehole is 10 m, the borehole of *S*, *L*, and *J* are arranged perpendicular to the construction surface. The borehole parameters are shown in tab. 2. Among them, the borehole *A* and *J* were fracturing holes during mining, which are used to solve roof collapse in upper corner of working face, *L* and *S* holes were fracturing holes before initial mining, and are used to solve roof collapse during initial mining.

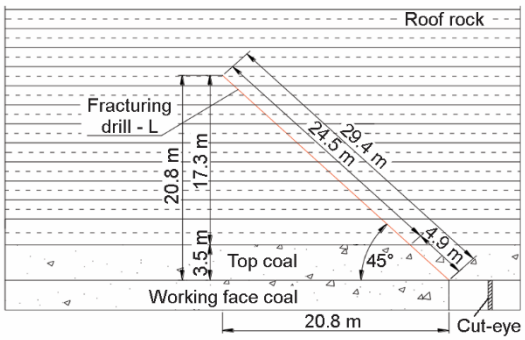

Figure 6. Borehole parameters of *S*

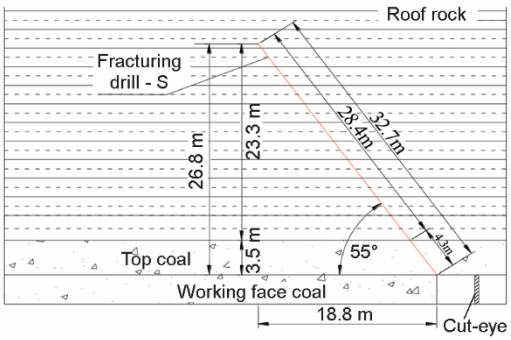

Figure 7. Borehole parameters of *L*

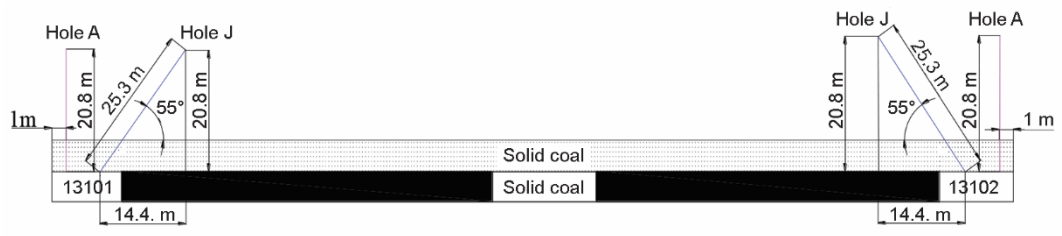

Figure 8. Fracturing borehole parameters of *J* and *A*

Table 2. Borehole design parameters

Borehole number	Azimuth [°]	Borehole depth [m]	Elevation [°]
S	133	32. 7	55
L	133	29. 4	45
A	223	25. 3	55
J	0	25. 3	55

The selection values of hydraulic fracturing pumps are:

– Previous studies have shown that the displacement of fracture opening mostly ranges from 1.2 mm to 2.2 mm, and the permeability of medium-grained sandstone varies from 70 mD to 100 mD [25-28]. In this calculation, the permeability is 100 mD, the fracture opening displacement is 0.002 m. The compressive strength of the main roof is 30.7 MPa, the cohesion is 6.73 MPa, and the internal friction angle is 36°36′.
– The third principal stress calculated by $\sigma_z = 0.0289H + 2.5462$. At present, the depth of coal seam is about 430 m, the value of σ_z calculated was 15.0 MPa, the initial fracture pressure is 0.1 MPa. According to the above parameters, the hydraulic fracturing pressure calculated by eq. (8). Through the above calculation, it is determined that the pressure of the fracturing pump should be greater than 28.1 MPa, and the selected model of the fracturing pump was 3ZSB80/62. The cracking pressure is related to the properties of coal and rock, and the maximum pressure is 40.0 MPa.

Results and discussion

Fracturing test data

There are 16 fracturing boreholes in 1310 fully mechanized caving faces setup room and two adjacent roadways. Each borehole begins to seal holes from the bottom of the hole and causes hydraulic fracturing once every 3 m intervals. Each hole causes hydraulic fracturing three times. The judging index of the end of hydraulic fracturing hole is that the water gushing around the hydraulic fracturing hole is obvious or the fracturing time is 30 minutes. The recorded pressure and injection time of the three-plunger pump are shown in fig. 9. It shows that the longest fracturing time of 16 hydraulic fracturing holes is 32 minutes, and the maximum water injection pressure of 12 of 16 hydraulic fracturing holes is over 28 MPa, which indicates that the hydraulic fracturing pressure calculation model is correct and the selection of hydraulic fracturing equipment is reliable. From 16 fracturing holes, 14 initial pressures are larger, which indicates that the pressure required for fracture initiation and propagation increases with the increase of the distance between fracturing section and aperture.

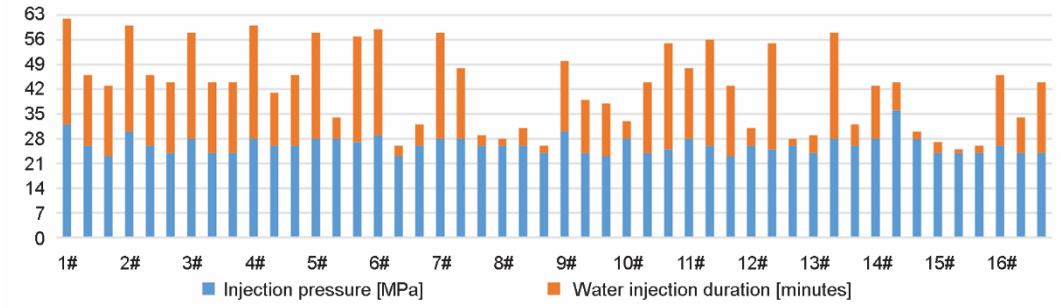

Figure 9. Parameters of water injection during the hydraulic fracturing

Investigation of fracturing effect

The roof began to collapse after 8 m advance, the roof weighting strength increased, and the immediate roof spanned a large area. According to calculation and previous experience, the first caving interval of immediate roof spanned about 8 m in 1310 working face. With advancing, three peak loads of support appear successively, the first peak occurs at 24 m of advancing face, the second peak occurs at 39 m of advancing face, the third peak occurs at 57 m of advancing face, the first and second peak intervals advance 15 m, and the second and third peak intervals advance 18 m. It can be concluded that the caving interval of first weighting of the main roof was 23 m and the caving interval of periodic weighting was 15-18 m. The caving interval of first weighting of main roof was reduced from 35 m to about 15-18 m after fracturing, which was similar to the caving interval of average weighting was 16 m, indicating that the effect of hydraulic fracturing is obvious. The strength of the first weighting of the main roof is reduced, which indicates that hydraulic fracturing controls the maximum area of the hanging roof in the goaf and realizes the safety management of the roof.

Roadway pressure monitoring

After adopting directional hydraulic fracturing, the average support resistance of support in working face is 2373.2 kN per frame, the average initial support force is 1898.6 kN per frame, and the average support strength of support is 0.767 MPa. The influence range of the advance abutment pressure on the working face is 25-30 m. The peak position is about 2-10 m in front of the coal wall, and the peak value is between 23-27 MPa. The measured average working resistance of the support before weighting accounts for 74% of the rated working resistance. After being affected by advance pressure during mining, the maximum displacement of two sides is 120 mm, the maximum displacement of roof and floor is 55 mm, the deformation of the roadway during the mining and the deformation during the excavation are up to 180 mm, and the maximum displacement of roof and floor is 86 mm. After the implementation of the project, the deformation of the roadway is small, and it is within the control range. The results show that the hydraulic fracturing technology can effectively block the transfer of lateral abutment pressure from the working face to the roadway and coal pillar, and solve the problem of large floor heave in the roadway.

Conclusions

By introducing the stress analysis and failure of rock mass, fracture development model and fluid seepage theory, the hydraulic fracturing initiation calculation model of roof is established, according to the calculation results of the model, the fracturing pump is selected, and the reliability of the model is verified by field industrial test.

According to the field conditions of coal mine, the fracturing parameters are designed. When fracturing the boreholes step by step, hydraulic fracturing can effectively expand the fracture in roof strata.

Directional hydraulic fracturing can make the roof of coal seam gradually collapse in different layers, effectively reduce the degree of roof pressure, the periodic weighting becomes not obvious. At the same time, the phenomenon of floor heave in adjacent roadways has been significantly suppressed, which shows that hydraulic fracturing has a good effect on controlling hard roof.

Acknowledgment

This work was supported by National Natural Science Foundation of China under the grant No. 51774116, and Postdoctoral Research Fund of Henan Province under the grant No. 001703031.

References

[1] Yu, B., *et al.*, Effect of Hard Roof Breaking on Gas Emission in Fully-Mechanized Sublevel Caving Mining of Extremely Thick Coal Seam, *Journal of China Coal Society*, *43* (2018), 8, pp. 2243-2249
[2] Fu, M. M., *et al.*, Research of the diSturbance of Curved Roof Caving for Gas in Upper Corner, *Journal of Mining & Safety Engineering in Chinese*, *33* (2016), 1, pp. 185-190
[3] Wang, J. C., *et al.*, Experimental Research on Gas Hazard Incident Caused by Roof Collapse, *Journal of Mining & Safety Engineering in Chinese*, *24* (2007), 1, pp. 8-12
[4] Chen, Y. G., *et al.*, *Strata Control Around coal Face in China, Xuzhou*, China University of Mining and Technology Press, Beijing, China, 1994
[5] Duzgun, H. S. B., Analysis of Roof Fall Hazards and Risk Assessment for Zonguldak Coal Basin Underground Mines, *International Journal of Coal Geology*, *64* (2005), 1/2, pp. 104-115
[6] Shi, Y. W., *et al.*, *Coal Face Surrounding Rock Control Principle and Technology (Volume II), Xuzhou*, China University of Mining and Technology Press, Beijing, China, 2003

[7] Papanastasiou, P., *et al.*, Influence of Inelastic Rock Behavior in Hydraulic Fracturing. In: Rock Mechanics in the 1990s (Volume I), (Bezalel Haimson Ed.), *Proceedings*, 34th U.S. Symposium on Rock Mechanics, University of Wisconsin, Madison, Wis., USA, 1993, pp. 339-342
[8] Murdoch, L. C., Mechanical Analysis of Idealized Shallow Hydraulic Fracture, *Journal of Geotechnical and Geoenvironmental Engineering*, *128* (2002), 6, pp. 488-495
[9] Yang, J. S., *et al.*, Experimental Study on Propagation Mechanism of Complex Hydraulic Fracture in Coal-Bed, *Journal of China Coal Society*, *37* (2012), 1, pp. 73-77
[10] Wu, Y. Z., *et al.*, Pressure Relief Mechanism and Experiment of Directional Hydraulic Fracturing in Reused Coal Pillar Roadway, *Journal of China Coal Society*, *42* (2017), 5, pp. 1130-1137
[11] Shi, X. Y., *et al.*, A Physical Simulation Experiment on Fracture Propagation of Coal Petrography in Hydraulic Fracturing, *Journal of China Coal Society*, *41* (2016), 5, pp. 1145-1151
[12] Liu, Y. W., *et al.*, Mechanical Frontiers in Shale-Gas Development, *Advances in Mechanics in Chinese*, *49* (2019), 1, pp. 201901-201901
[13] Yan, S. H., *et al.*, The Mechanism of Hydrobreakage to Control Hard Roof and Its Test Study, *Journal of China Coal Society*, *25* (2000), 1, pp. 32-35
[14] Kang, H. P., *et al.*, Monitoring of Stress Change in Coal Seam Caused by Directional Hydraulic Fracturing in Working Face with Strong Roof and Its Evolution, *Journal of China Coal Society*, *37* (2012), 12, pp. 1953-1959
[15] Kaiser, P. K., *et al.*, Design of Rock Support System Under Rock Burst Condition, *Journal of Rock Mechanics and Geotechnical Engineering*, *4* (2012), 3, pp. 215-227
[16] Banerjee, G., *et al.*, Hard Roof Management – A Key for High Productivity in Longwall Coal Mines, *Journal of Mines, Metals and Fuels*, *51* (2003), 7, pp. 238-244
[17] Sneddon, I. N., The Distribution of Stress in the Neighborhood of a Crack in an Elastic Solid, *Proceedings A*, *187* (1946), 1009, pp. 229-260
[18] Nordgren, R. P., Propagation of a Vertical Hydraulic Fracture, *Society of Petroleum Engineers Journal*, *12* (1972), 4, pp. 306-314
[19] Khristianovich, S. A., *et al.*, Formation of Vertical Fractures by Means of Highly Viscous Liquid, *Proceedings*, 4th World Petroleum Congress, Rome, Italy, 2, 1995, pp. 579-586
[20] Geertsma, J., *et al.*, A Rapid Method of Predicting Width and Extent of hydraulically Induced Fractures, *Journal of Petroleum Technology*, *21* (1969), 12, pp. 1571-1581
[21] Lin, B. Q., *et al.*, Research on Dynamic Characteristics of Hydraulic Fracturing in Coal Body Containing gas, *Journal of Mining & Safety Engineering in Chinese*, *29* (2012), 1, pp. 106-110
[22] Chernov, O. I., *et al.*, Oriented Hydraulic Fracturing of a Mass of Rocks Enclosing the "International" Diamond Pipe, *Journal of Mining Science*, *33* (1997), 6, pp. 582-586
[23] Joon-shik, M., Representativeness of Jointed Rock Mass Hydraulic Conductivity Obtained from Packer Tests for Tunnel Inflow Rate Estimate, *International Journal of Rock Mechanics and Mining Sciences*, *48* (2011), 5, pp. 836-844
[24] Huang, B. X., *et al.*, Theory and Technology of Hydraulic Fracturing for Controlling Hard Roof of Underground Mining, *Chinese Journal of Rock Mechanics and Engineering*, *36* (2017), 12, pp. 1-17
[25] Cai, F., *et al.*, Simulation and Experimental Research on Upward Cross-Seams Hydraulic Fracturing in Deep and Low-Permeability Coal Seam, *Journal of China Coal Society*, *41* (2016), 1, pp. 113-119
[26] Kurlenya, M. V., *et al.*, Stimulation of Underground Degassing in Coal Seams by Hydraulic Fracturing Method, *Journal of Mining Science in Chinese*, *53* (2017), 6, pp. 975-980
[27] Jeffrey, R., *et al.*, Sand Propped Hydraulic Fracture Stimulation of Horizontal In-seam Gas Drainage Holes at Dartbrook Coal Mine, *European Journal of Radiology*, *37* (2004), 1, pp. 8-17
[28] Patutin, A., *et al.*, Transverse Hydraulic Fracture Initiation by Indentation in an Uncased Borehole, *Procedia Engineering*, *191* (2017), Dec., pp. 287-290

Paper submitted: November 4, 2019
Paper revised: May 20, 2020
Paper accepted: May 20, 2020